An Acad Bras Cienc (2022) 94(Suppl. 1): e20210800 DOI 10.1590/0001-3765202220210800
Anais da Academia Brasileira de Ciências | *Annals of the Brazilian Academy of Sciences*
Printed ISSN 0001-3765 I Online ISSN 1678-2690
www.scielo.br/aabc | www.fb.com/aabcjournal

GEOSCIENCES

Lagged response of Tropical Atlantic Ocean to cold and fresh water pulse from Antarctic sea ice melting

ANA LAURA R. TORRES, CLAUDIA K. PARISE, LUCIANO P. PEZZI, MICHELLY G. DOS SANTOS QUEIROZ, ADILSON M.B. MACHADO, GABRIEL S. CERVEIRA, GUSTAVO S. CORREIA, WESLEY L. BARBOSA, LEONARDO G. DE LIMA & UESLEI A. SUTIL

Abstract: The formation of dense water masses at polar regions has been largely influenced by climate changes arising from global warming. In this context, based on ensemble simulations with a coupled model we evaluate the meridional shift of a climate signal (i.e., a cold and fresh water input pulse generated from melting of positive Antarctic sea ice (ASI) extremes) towards the Tropical Atlantic Ocean (TAO). This oceanic signal propagated from Southern Ocean towards the equator through the upper layers due to an increase in its buoyance. Its northward shift has given by the Subantarctic Mode Water (SAMW) and Antarctic Intermediate Water (AAIW) flows, that inject cold and fresh mode/intermediate waters from into subtropical basin. The signal has reached low latitudes through the equatorial upwelling and spreads out southwards, through the upper branch of southern subtropical gyre. We concluded that 10 years of coupled simulations was enough time to propagate the climate signal generated by ASI positive extremes melting, which reached TOA around 2 year later. The oceanic connection between Southern Ocean and TAO is indeed established within the timescale analyzed in the study (10 years). Nonetheless, the period needed to completely dissipate the disturbance generated from ASI seems to be longer.

Key words: Sea Ice Melting, Freshwater Input, Teleconnections, Oceanic Bridge, Oceanography.

INTRODUCTION

Considered as one of the early indicators of global warming through the months when sea ice typically reaches its minimum and maximum extent, the Antarctic sea ice (ASI) has a great influence on the heat balance in Earth, since it acts as a natural thermal insulator on the ocean surface (Eicken et al. 1995, Maksym et al. 2012, Parise 2014). Besides affecting the heat and mass exchanges between sea ice and ocean and sea ice and atmosphere, the ASI also acts directly on the formation of important water masses responsible for the global thermohaline circulation, such as the Antarctic Bottom Water (AABW) and the North Atlantic Deep Water (NADW) (Toggweiler & Samuels 1995, Nadeau et al. 2019). Therefore, due to intrinsic characteristics of the sea ice, the impacts of the current scenario of global warming have been amplified in polar regions (Thomas & Dieckmann 2010, Stuecker et al. 2018, Casagrande et al. 2020).

The low-frequency oscillations analysis brings a broad view of the propagation of planetary wave trains, so that local forces end up influencing remote regions of the globe via oceanic or atmospheric teleconnections. Thus,

the identification of teleconnection mechanisms is useful in the diagnostic studies and prognostics of climate anomalies (Stammerjohn et al. 2012), such as those associated with extreme ASI advance or retreat events (Massom et al. 2008, Massom & Stammerjohn 2010, Raphael et al. 2011, Parise et al. 2015). The study of teleconnections, in addition to provide information on the possible triggers and mechanisms, enables the understanding of causes and effects in climate studies (Wallace & Gutzler 1981, Liu et al. 2002, Purich & England 2019). Through teleconnection modes that arise from the natural internal variability of the coupled climate system, the sea surface temperature (SST) of the Tropical Atlantic Ocean (TAO) has its patterns changed by the passing of atmospheric planetary wave trains (Li et al. 2015), ending up directing the meridional positioning of the Atlantic Intertropical Convergence Zone, with severe impacts on the precipitation of the northern and southern regions of South America (Giannini et al. 2001, Wu et al. 2007, Chiang et al. 2008).

Since it is essential to identify the mechanisms that influence the internal variability of lower frequency oscillations between remote regions of the globe, analytical performance becomes necessary for a better understanding of this dynamical system. With this in mind, coupled climate models have become increasingly important in climate change studies, given their ability to simulate global and regional variability (Randall et al. 2007, Flato et al. 2013). Parise et al. (2015) analyzed the sensitivity and memory of the Southern Hemisphere climate under ASI positive extremes through ensemble simulations performed with a climate model. According to these authors, the Southern Ocean has a climate memory of ~ 4 years to the ASI extremes, in both concentration and thickness, imposed as the initial condition in the sensitivity experiments performed. After this time, the melting freshwater pulse has persisted for the following 4 years over the Southern Ocean surface under current climate conditions. Even after all the imposed ice been melted, a cold and fresh water persisted at surface of the Southern Ocean, continuing to influence the vertical heat fluxes. After the period of 8 years of model simulation, a reduction in ASI was observed compared to the control simulation, as a result of the heat release stored at the subsurface layers of the Southern Ocean. As soon as the extreme applied to the ASI has melted, the cold and fresh water resulting from it advanced northwards. As a consequence, the Southern Ocean started to transfer heat back to the atmosphere (Parise et al. 2015). These authors concluded that the restoring of the climate thermal balance is triggered by a two distinct timescale mechanism, which is initiated by the insulating effect of sea ice and the resulting pulse of cold and fresh water (rapid response) and restored by the heat stored in the subsurface layers of the Southern Ocean as the cold and fresh surface water is transported towards the lower-latitudes (slow response). A similar mechanism was found and discussed by Ferreira et al. (2015).

Based on the information provided by Parise et al. (2015), the hypotheses of this study were elaborated. Given the answers found by Parise, together with the mechanism that showed the impacts on the atmosphere and the Southern Ocean, one of the questions generated was whether this climate signal was transferred via the ocean to the TAO, how this transport would occur, in what magnitude and how long it would take for it to arrive. Thus, this study aims to complement the answers found by Parise et al. 2015. A decades-long satellite-based study revealed that the gradual increase in the ASI extents has reversed in 2014, with subsequent rates of decrease from 2014 to

2017, far exceeding the more widely decay rates experienced in the Arctic (Parkinson 2019). In 2017, the rapid decreases reduced the ASI extents to their lowest values in the 40 years record of observations, presenting both a new yearly (2017) and monthly (February) record low. However, the fact that the ASI decreases during this short period does not assurance that the 1979–2014 overall positive trend in Southern Ocean ice extents has reversed to a long-term negative trend (Parkinson 2019). The last two positive records of ASI extent have also occurred recently, in September 2013 (19.77×10^6 km^2) and October 2014 (20.11×10^6 km^2) (NOAA 2014).

Under the scenario of global warming, it is of great interest to understand the impacts of ASI extremes in the TAO, since this oceanic region has large impacts on the climate of the north and northeast regions of Brazil (Pezzi & Cavalcanti 2001, Yoon & Zeng 2010, Utida et al. 2019) and houses important coral reef formations, such as the Amazonian and Manoel Luís Reefs (Moura 2016). Thus, we study the impacts and the lagged response of the TAO to the climate signal generated from southern high latitudes due to the increasing in area and volume of ASI. The northernmost latitude impacted and the mechanisms that act on the propagation via oceanic teleconnections of this climate disturbance from Antarctica to the TAO are also studied.

CLIMATE DATA AND NUMERICAL EXPERIMENTS

The ocean temperature and salinity data used in this study were obtained from two ensemble simulations performed with 30–members each, using the Coupled Climate Model version 2.1 (CM2.1; Delworth et al. 2006) developed at the Geophysical Fluid Dynamics Laboratory (GFDL). The CM2.1 model can simulate the climate system from weather to climate change scales without using flux adjustment to maintain a stable climate (Parise et al. 2015). It is composed of four separate (atmosphere–land–ocean–sea ice) components that interact with each other through the Flexible Modeling System coupling system. The ocean component of CM2.1 model is the version 5.0.2 of the Modular Ocean Model (Griffies et al. 2000). The sea ice component is a multi-layer sea ice model that resolves rheological processes of ice such as internal stresses and its resulting deformations, making it more dynamic in its heat and salt exchanges at sea ice-atmosphere and sea ice-ocean interfaces (Parise et al. 2015).The ensemble experiments (hereafter named as *layerctl* and *layermax*) were configured to assess the sensitivity of the Southern Hemisphere's climate to a historical maximum condition in ASI under the current climate conditions, for a period of 10 years (from July 2020 to June 2030, Table I). The initial conditions for the both ensemble experiments were derived from a control run of 10 years forward from a spin-up run, where the climate conditions for each July–August–September (JAS) were used. This procedure has saved the climate conditions as close as possible to the period of the seasonal ASI maximum (September) and also includes the interannual variability of the climate by saving the JAS period for the first year, second year, third year, and so on. These 30 (10 years x 3 months; middle–late winter and early spring) climate conditions were used as initial conditions for the ensemble experiments, which were initialized in the month of July. Except for the ASI maximum fields, the ensemble initial conditions were the same for all experiments (Table I). The maximum concentration of ASI, in turn, was calculated from the Met Office Hadley Center data set (HadISST1, 1870–2008) (Rayner et al. 2003), while the maximum thickness was calculated from a monthly climatology provided

Table I. Schematic table with basic information on the sensitivity experiments performed with the CM2.1 model and used in this study, as a complement to that presented by Parise et al. (2015).

	layerctl	layermax
Horizontal and vertical resolution of the oceanic component	1° in latitude and 1° in longitude, this latter getting progressively finer toward the equator (0.33° resolution), with 50 z-coordinate levels	
Model spin-up	a short (1 year) uncoupled simulation, with only the ocean and sea ice models, followed by a long (30 years) fully coupled integration, from 1990 to 2020	
Initial conditions for ASI concentration (%)	a control model integration of 10 years forward from the spinup, where the restarts conditions for each July–August–September (JAS) were used	Met Office Hadley Center dataset, from 1870 to 2008 (Rayner et al. 2003)
Initial conditions for ASI thickness (m)		GFDL monthly climatology from 1979 to 1996 (Taylor et al. 2000)
Running-period (Parise, 2014)	10 years, from July 2020 to June 2030	
Running-period analyzed in the presente study	the same of Parise (2014) and also following the predetermined periods by Parise et al. (2015) in relation to the ASI *layermax-layerctl* differences: the positive phase (July 2020–June 2024); the near–to–zero phase (July 2024–June 2028) and the negative phase (July 2028–June 2030)	

by the GFDL (1979–1996) (Taylor et al. 2000). Both conditions (area and volume) represented the maximum value of sea ice in the time series for each grid point, regardless of when it has occurred in time (Supplementary Material, Figure S1). More details about configuration and performance of the sensitivity experiments used in the present study can be seen in Parise (2014) and Parise et al. (2015).

Firstly, the annual mean biases of the *layerctl* experiment were evaluated for the TAO domain through the comparison with the Simple Ocean Data Assimilation version 3.3.1 (SODA; Carton et al. 2018) oceanic reanalysis database (2006–2015). To measure the seasonal differences between two time series, the metric of Root Mean Square Error (RMSE) was used, as defined below according to Hyndman & Koehler (2006) and Chai & Draxler (2014):

$$RMSE = \sqrt{\sum_{i=1}^{n} \frac{(\hat{y}_i - y_i)^2}{n}}$$

where $\hat{y}_i$ are the predicted values, y_i are the observed values and n is the total number of observations.

Then, the impacts of ASI changes on TAO were evaluated for the whole simulated period (2020–2030) and also separately for three predetermined periods based on the criteria established in Parise et al. (2015): from July 2020 to June 2024 when the ASI differences (*layermax–layerctl*) were still positive; from July 2024 to June 2028 when the ASI differences were close to zero; and from July 2028 to June 2030 when the differences were negative, that is, the ASI coverage became larger in the control experiment (*layerctl*) compared to the experiment that has received the disturbance (*layermax*).

The propagation time of the climate signal from high to low latitudes was here analyzed through Hovmöller diagrams (latitude *vs* time) for the ocean temperature and salinity. These were obtained by calculating their zonal and vertical means in order to show the meridional propagation (Antarctica–Tropics) of the disturbance over time. In order to know through of which layer in the TAO the largest meridional transport of heat and mass has occurred, an average vertical profile (latitude *vs* depth) was obtained over time for the predetermined periods studied here (i.e., July 2020–June 2024; July 2024–June 2028; and July 2028–June 2030).

RESULTS

Meridional shift of the climate sign generated from Antarctica

Our results are all based on the differences between the *layermax–layerctl* ensemble experiments means. The largest SST and SSS changes faced to ASI positive extremes have occurred during the middle–late spring to early-middle summer (Oct–Nov–Dec–Jan) (Figure 1). In general, the ASI positive extremes have resulted in a cold (-0.8°C) and fresh (-0.2) water anomalous pulse from the Antarctica to the north (Figure 1a–b). The main SST and SSS changes in the Southern Ocean have propagated from the sea ice edge (60°S–70°S), where the

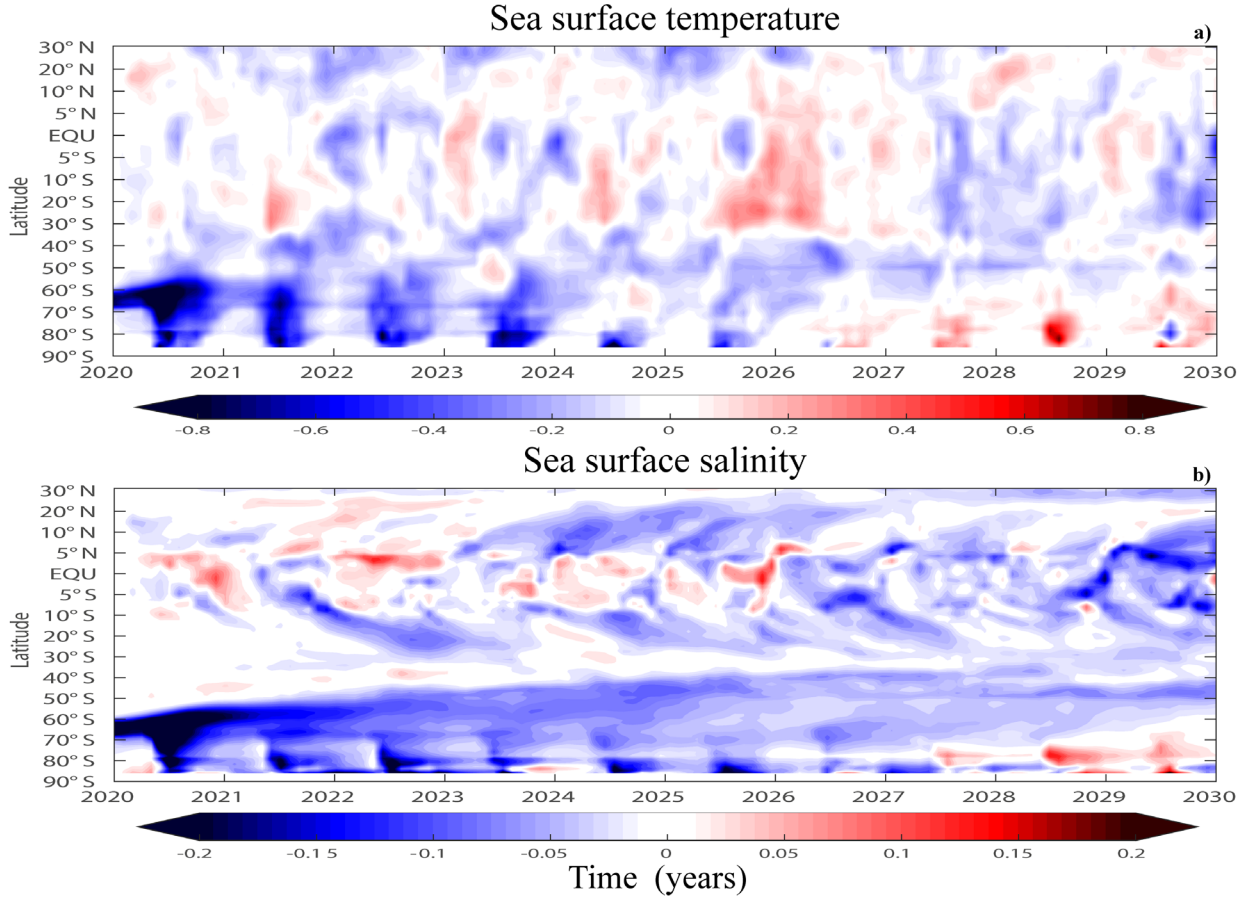

Figure 1. Hovmöller diagrams for the zonal mean of (a) sea surface temperature (SST, in °C) and (b) sea surface salinity (SSS) differences (*layermax–layerctl*) in the Atlantic sector for the period simulated from July 2020 to June 2030.

intensified heat and salt fluxes contribute to sea ice melting (Parise 2014), towards the TAO (Figure 1a). Near the Antarctic continent, the SST biases were larger during the melting seasons (southern summer and autumn), once during the freezing seasons the ASI coverage is also large in control (climatological) simulation. As the cold bias propagates towards the equator, warmer biases are observed over the southern high latitudes (Figure 1a, since 2027). Although some changes in SST can be found in certain regions of the southern TAO, a large warm bias has occurred in this from 30°S to 20°N in the sixth year of simulation, indicating an intensification of both subtropical oceanic gyres, especially in the southern cell (Figure 1a, in 2026). In the last 2 years, the southern TAO presented a cold bias, that became even larger in the end of simulation (-0.4°C). This indicates that, in terms of TAO response to ASI extremes, 10 years of coupled simulation was not time enough to completely dissipate the resultant climate signal.

The impacts of ASI positive extremes on sea surface salinity (SSS), in turn, were persistent along the yearly cycle in the Southern Ocean, with the fresh water continually propagating from Antarctica towards the tropics, reaching 30°S at the end of the fourth year of simulation (Figure 1b). Near the equator (5°S–5°N), SST changes have appeared firstly as a dipole structure, with a fresher (saltier) bias in southern (northern) sector, respectively (Figure 2, from 2020 to 2021). Then, the equatorial fresh biases start to move southwards, spreading the freshwater over the southern tropical latitudes (until 30°S). It seems that SSS biases found in southern high latitudes do not reach the low latitudes by the ocean surface of Southern Hemisphere, once they have appeared there before the freshwater pulse has reach the parallel of 30°S, as we will discuss forward. The response of SSS to ASI positive extremes has also shown the intense action of meridional teleconnections in TAO, which propagated especially from low to mid latitudes until the end of simulation (Figure 1b).

The ocean temperature and salinity biases found through the zonal (from 90°S to 30°N) profiles (0 to 500 m) during the predetermined periods (i.e., July 2020–June 2024; July 2024–June 2028; and July 2028–June 2030) are showed in Figures 2 and 3. During the first 4 years of simulation, the ASI positive extremes resulted in cold biases (-0.4°C) in the upper layers of Southern Ocean, from south pole to 30°S, and more intensely south of 50°S (Figure 2a, in blue). As the same time, warm biases (+0.4°C) are found occurring just below 50 m, in subsurface layers of southern high latitudes (Figure 2a, in red). The cold biases have moved towards the mid latitudes during the following 4 years of model integration, with the largest changes occurring around 50°S, over the Antarctic Convergence (Figure 2b). As the cold water is displaced towards the equator by the enhanced Ekman transport in mid latitudes (Parise 2014), the warmer subsurface water is allowed to exchange heat fluxes with the southern atmosphere again (Figure 2c). Still in the last 2 years of the experiments, the cold bias is found spreading over the mixed-layer of the whole TAO (Figure 2c). Before the climate signal is spread over the surface, cold biases are found over the southern subtropics, indicating a weakening of the oceanic gyre. We also observed a cold bias around 30°N, from surface to 200 m depth, whose changes can be related to Mediterranean Intermediate Water flow (Giorgi & Lionello 2008). This is associated with a slight subsurface warming (+ 0.1°C) in the northern TAO, first in 20°N (Figure 2a) and last in 10°N (Figure 2c).

Negative biases of ocean salinity (~ -0.2) from the surface down to approximately 80 m depth were found over southern mid and high latitudes during the first 8 years of model

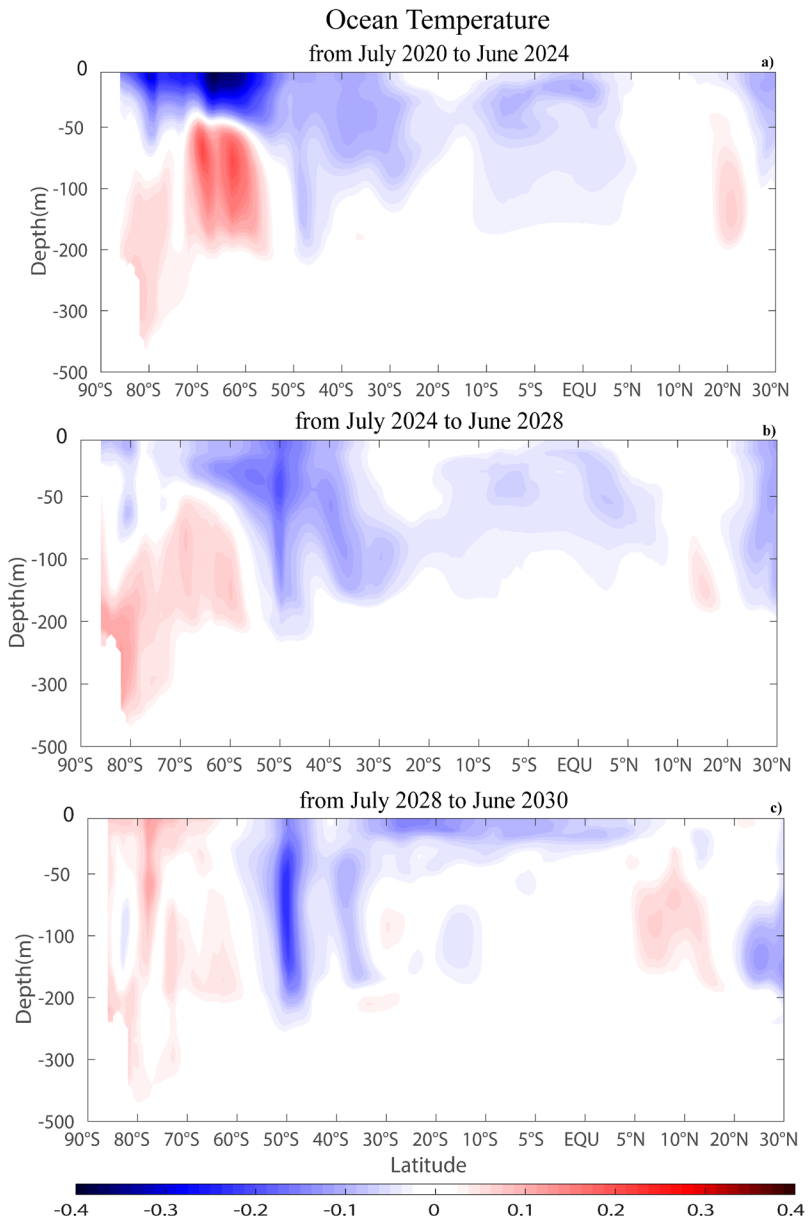

Figure 2. Zonal mean vertical (0–500 m) profile of ocean temperature differences (*layermax–layerctl*) extending from 90°S to 30°N during the periods: **a)** July 2020–June 2024; **b)** July 2024–June 2028 and **c)** July 2028–June 2030.

simulation (Figure 3a–b). In the first 4 years, the fresh bias extends until the latitude of 50°S (Figure 3a) and up to 40°S for the next 4 years (Figure 3b). Then, the fresh biases have spread out all over the whole Atlantic surface, except over the southern high latitudes where a saltier bias is found (-0.05). The fresher water peaks at 50°S and also at 4°N, both from the surface to 110 m depth (Figure 3c).

In short, our study has shown that the melting-resulted cold and fresh water has been shifted from the Southern Ocean towards the low latitude through the Subantarctic Mode Water (SAMW) flow, in the upper ocean layers (0–50m). At the Antarctic Convergence (50°S), this climate signal eventually influences the Antarctic Intermediate Water (AAIW) flow by buoyancy gain, once it has resulted from the melting of ASI extremes. The low salinity core of AAIW extends northwards from the Antarctic Polar Front zone at a depth of about 1000 m beneath the subtropical gyres (Sloyan & Rintoul

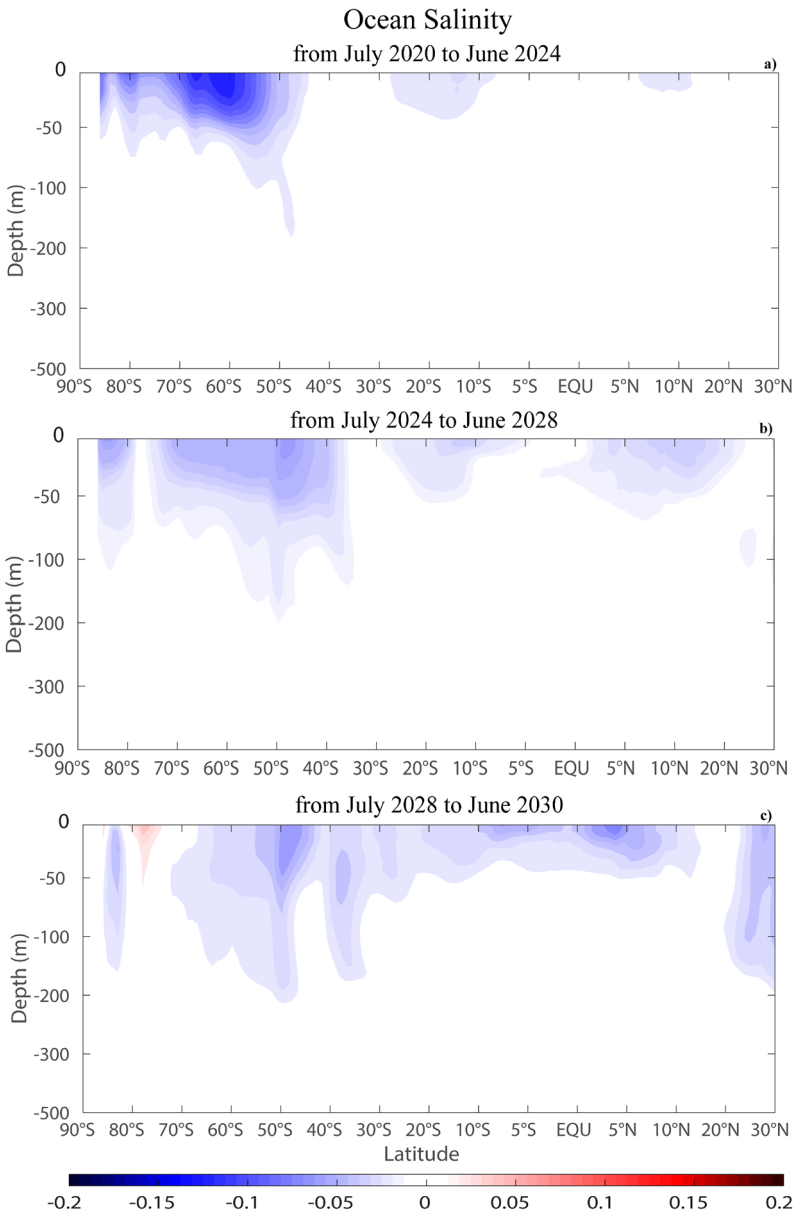

Figure 3. Zonal mean vertical (0–500 m) profile of ocean salinity differences (*layermax–layerctl*) extending from 90°S to 30°N during the periods: a) July 2020–June 2024; b) July 2024–June 2028 and c) July 2028–June 2030.

2001). Here, the increased AAIW flow became shallower, eventually modifying the whole subtropical cell (Figure 2a–b).

Response of tropical atlantic ocean to positive extremes applied to Antarctic sea ice field

From this section onwards, we started to show the results from our study obtained through numerical modeling experiments of climate, when extremes ASI were imposed as initial conditions for each ensemble member. First, the performance of the GFDL/CM2.1 model in simulating the TAO surface fields was evaluated. The results from RMSE show that the SST (SSS) fields in the TAO are better simulated by CM2.1 model during MJJ (NDJ and DJF quarters) quarters, respectively (Table II). For SST, the largest errors were found in the middle of year (AMJ), while for SSS they occurred in the beginning of the year (MAM) (Table II).

Table II. Seasonal RMSE between *layerctl* ensemble experiment (2020–2030) and SODA3.3.1 reanalysis (2006–2015) for sea surface temperature (SST, in °C) and sea surface salinity (SSS).

	QUARTERS											
	DJF	**JFM**	**FMA**	**MAM**	**AMJ**	**MJJ**	**JJA**	**JAS**	**ASO**	**SON**	**OND**	**NDJ**
SST	0.41	0.40	0.38	0.34	0.31	0.90	0.62	0.34	0.38	0.37	0.33	0.32
SSS	0.18	0.16	0.13	0.09	0.11	0.12	0.13	0.11	0.11	0.14	0.16	0.18

Through the *layermax–layerctl* differences for the ocean fields simulated by the GFDL/CM2.1 model we found that temperature and salinity of the TAO are sensitive to the ASI extremes, as following details. The average profile (time x depth) for the ocean temperature differences calculated from the spatial average in the TAO domain (from 30°S to 30°N) clearly showed a cold bias (-0.15°C) from the surface down to 150 m depth approximately (Figure 4a). This has become more intense at surface after 2 years of simulation (2022), being deepened in the following year (2023). This subsurface signal has persisted for the next 4 years (2024–2027), when it is weakened. That is associated with a warm bias (+ 0.15°C) near the surface from 2026 to 2027. Afterwards, the climate signal propagated as an oscillatory pattern that alternated between cold and warm waters in the first layers of ocean (0–50 m). When the cold bias dominated the superficial layers of the TAO in 2027, it was associated with a warm bias (+ 0.01°C) at subsurface layers in the following year (Figure 4). It is also noted that the disturbance applied to the ASI field was not fully dissipated after the 10th year of model simulation, which was evaluated in this study.

The time x depth mean profile for the TAO salinity is shown in Figure 4. The result shows that TAO presented a small (-0.01) but persistent fresh bias at the surface of the experiment *layermax* compared to *layerctl*. The superficial (upper to 100 m) fresher biases were larger after 2 years of simulation (from 2022) and have persisted until the end of the experiment. This indicates that 10 years of simulation was not time enough to dissipate the climate signal generated by ASI positive extremes, which has propagated northwards as cold and fresh water, first at surface and then through sub-superficial layers (Figure 4b).

DISCUSSION

The cold and fresh water pulse found in the present study as a result of melting ASI extremes has moved towards the TAO through the SAMW flow (Sloyan & Rintoul 2001). This water mass is usually formed on the northern face of the Antarctic Polar Front and then transported to the South Atlantic and North Atlantic basins (Williams et al. 2006). As the subsurface Antarctic waters flow northwards, warm subtropical waters are taken southward to replace them. The subsurface cooling mitigates an intensification of the subtropical gyre which is linked to the transport from the AAIW and SAMW water masses that naturally inject cold and fresh water into the subtropical basins, where together with the South Atlantic Current feeds the gyre, strengthening it (Jacobs et al. 2002, Curry et al. 2003).

In the period when the ASI was still higher in comparison to the control simulation (first 4 years of simulations), the condition was associated to the freshwater input into the

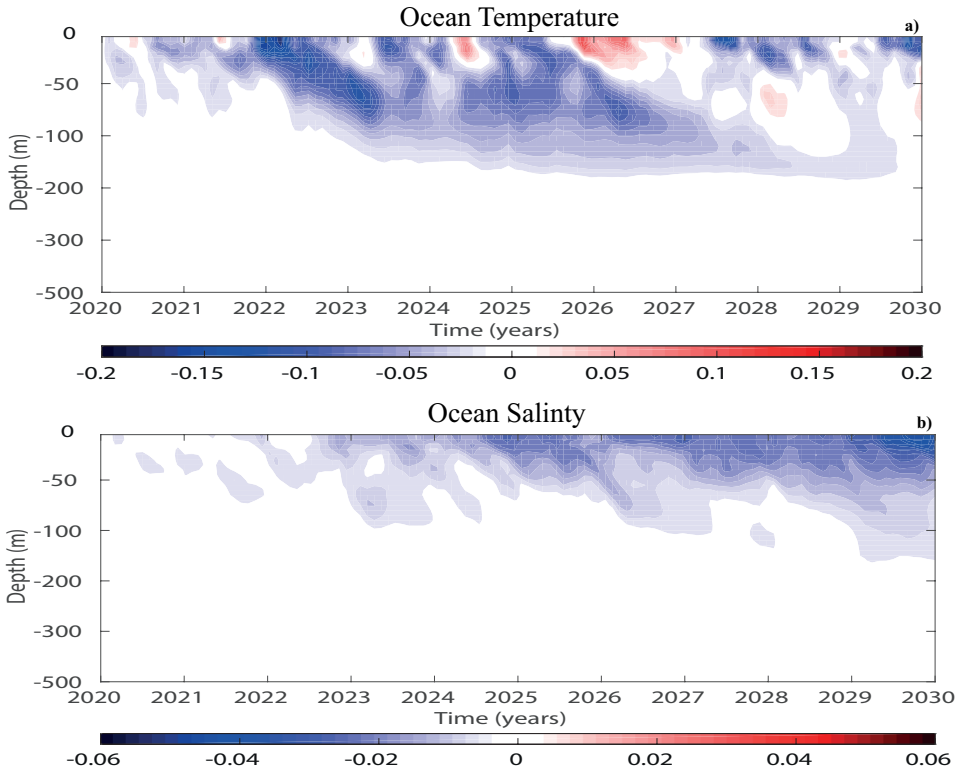

Figure 4. Time x depth (0–500 m) mean profile of (a) ocean temperature and (b) salinity differences (*layermax–layerctl*) from the spatial average in the TAO domain (30°S–30°N), during the 10 years of model simulation (July 2020–June 2030).

Southern Ocean (Parise et al. 2015), that was transported northwards by intensified flows of Antarctic superficial waters. Such freshening of the upper Southern Ocean is responsible for a reduction in the AAIW salinity (Curry et al. 2003). Reduced salinity implies an enhanced freshwater input on the ocean surface, and normally is associated with increase of precipitation, sea ice melting, ice shelves melting, ice sheets and glaciers melting, and also changes in oceanic processes, such as reduced upwelling of Lower Circumpolar Deep Water (Cook et al. 2005, Carter et al. 2008).

The freshwater exchange between sea ice and ocean has a substantial influence on deep ocean heat uptake in the Southern Ocean (Kirkman & Bitz 2011). According to these authors, the freshwater input mainly from sea ice reduces the convection process, which in turns reduces the entrainment of heat into the mixed-layer and reduces the upward heat transport along isopycnals. The reduced upward heat transport causes deep-ocean heating south of 60°S and below 500–m depth, with a corresponding surface cooling in large parts of the Southern Ocean. These results indicate that changing sea ice freshwater and salt fluxes are key component in the surface warming of the Southern Ocean and the weak reduction in ASI in model projections (Mackie et al. 2020).

The northward melting freshwater transport implies on changes in the ocean salinity of waters entering the lower and upper overturning cells. This process of northward freshwater transport by sea ice effectively removes freshwater from a region making up the lower overturning cell, in particular AABW, and adds freshwater to the upper circulation cell, especially AAIW (Haumann et al. 2016). Therefore, as the salinity dominates the density structure in polar oceans, the sea ice changes and the meridional transport of melting-resulted freshwater are the major contributors to recent salinity changes in the Southern Ocean. The mid-depth

salinity minimum layer characterizing the AAIW is one of the most prominent features of the Southern Hemisphere oceans. The low-salinity core extends northwards from the Antarctic Polar Front zone at a depth of about 1000 m beneath the subtropical gyres in each basin. In the Atlantic, the AAIW core can be traced across the equator and into the North Atlantic, where it supplies a large fraction of the northward flow required to balance the export of North Atlantic Deep Water (Schmitz & Richardson 1991). Using satellite observations supplemented by sea-ice reconstructions, the authors still estimated that the wind-driven northward freshwater transport by sea ice increased by 20±10 per cent between 1982 and 2008 (+6± 3 mSv decade-1). This enhanced divergence of sea ice and freshwater may also result from a maximum of ASI, followed by its melting and freshwater pulse into the Southern Ocean, as shown in our study.

Early studies suggested that the circumpolar formation of AAIW is resulted from the sinking of Antarctic Surface Water below the Subantarctic Front (Deacon 1937). This circumpolar formation mechanism was essentially replaced by theories that suggest the formation of AAIW is explicitly linked to SAMW, instead of to Antarctic Surface Water (McCartney 1977) and that the renewal of AAIW occurs in specific regions of the Southern Ocean, such as the southwest Atlantic sectors (Georgi 1979, Molinelli 1981, Piola & Georgi 1982, Piola & Gordon 1989).

The SAMW and AAIW are important linkage ways from Antarctica to tropical regions since they act as main conduits for the supply of ocean proprieties. After being formed in the Southern Ocean these mode and intermediate waters are transported eastward with the Antarctic Circumpolar Current and northward into the adjacent subtropical gyres. In the Atlantic Ocean, SAMW and AAIW initially move northward with Malvinas Current adjacent to South American continent, but its penetration into the subtropical gyre along the western boundary is blocked by the southward flow of the Brazil Current (see forward in Figure 5). SAMW and AAIW are eventually transported into the subtropical gyre at the eastern boundary when part of the South Atlantic Current turns northward, feeding the Benguela Current (Stramma & Peterson 1990, Peterson & Stramma 1991). The northward currents transport of SAMW and AAIW from South Atlantic oceans injects cold, fresh mode and intermediate waters into the subtropical ocean basin. SAMW and AAIW circulate in the wind-driven gyres on each subtropical basin. In the western Brazil, Agulhas, and East Australian currents, modified warm, salty mode and intermediate waters are returned to the Southern Ocean. The exchange of 'new' mode and intermediate water with 'older' mode and intermediate water represents the mechanism by which Antarctic upper waters ventilate the subtropical gyres (Sloyan & Rintoul 2001).

Our results also show a reduction in the TAO salinity from the fourth year of simulation (2024), just when the ASI field returns to its climatological condition. After that period, even though ASI field has already returned to its climatological state, a climate memory to the initial conditions of sea ice has persisted for the next four years (until 2028) as an input pulse of cold and fresh water into the Southern Ocean (Parise et al. 2015). This was transported northwards by the SAMW flow, through the oceanic upper layers, in response to increased Ekman transport in mid latitudes (Parise 2014). The decrease in TAO temperature and salinity just below the mixed-layer (from 100 to 700 m) suggests an intensification of the shallow Subtropical Cell (STC), which consists of a warm Ekman flux at the surface towards the pole. In compensation, the STC provides cold source

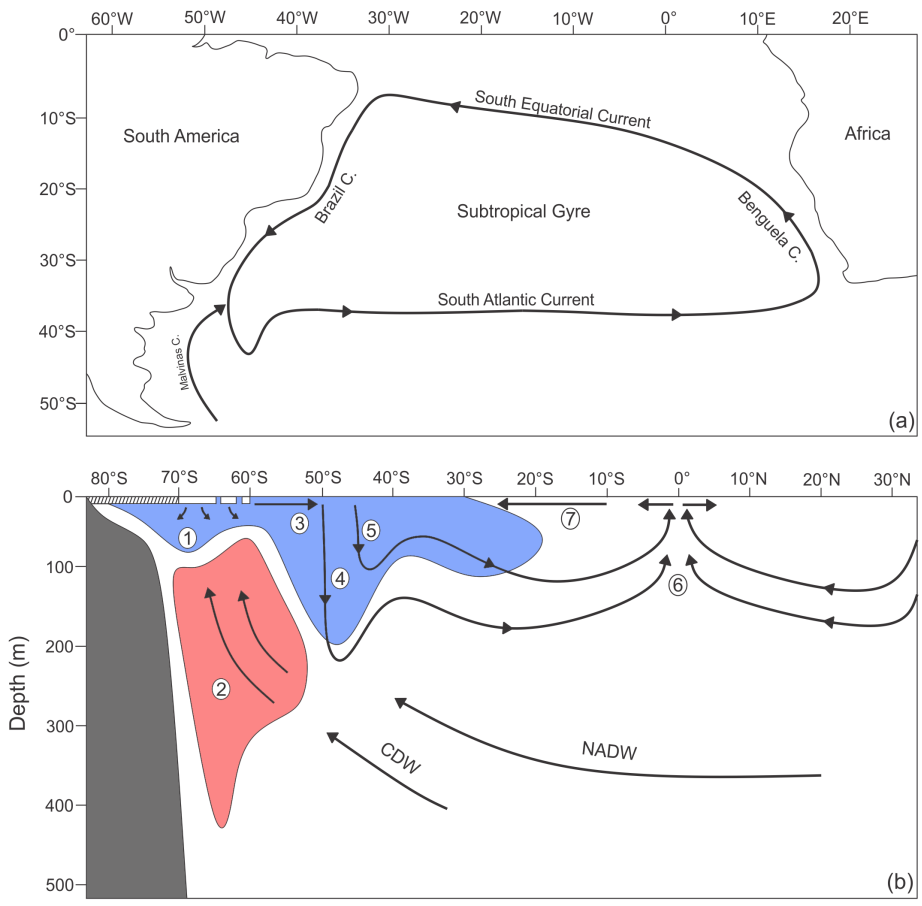

Figure 5. Schematic of the main changes in Southern Ocean and of how the cold and fresh water pulse from Antarctic sea ice melting has transferred towards the Tropical Atlantic Ocean.

waters towards the equator, like an oceanic signal bridge (Kröger et al. 2005).

It is known that the rate of global ocean water masses formation and transport are limited not only by the efficiency of high latitude convective mixing, but also by the southern density gradient (pole-tropics) and the ability of the ocean to heat up the deep waters that emerge (Bryan 1987, Marotzke & Scott 1999). The larger stratification of the Southern Ocean has resulted from salinity changes related to melting of ASI extremes. Increased stratification in the surface layers has also reduced the ability of ocean to lose heat to the atmosphere, resulting in a warming in the subsurface layers of the Southern Ocean (Parise et al. 2015). As a consequence, the subduction processes of water masses under a stratified ocean are generally suppressed (Bitz et al. 2006, Aiken & England 2008).

In addition to the sea ice cover, the colder surface of the ocean also affects the atmosphere by providing less heat fluxes transfer (Pezzi et al. 2009, 2016 and 2021, Parise et al. 2015). At mid latitudes, the air temperature decreases and the westerly winds decrease from 45°S to 60°S and intensify from 30°S to 45°S in response to increased ASI (Raphael et al. 2011). According to Parise et al. (2015), the more intense the interactions between sea ice and the other components of the coupled climate system, the faster the maximum anomalies imposed on the ASI field melts, and consequently the larger the input of cold and fresh water into the Southern Ocean. This ocean-sea ice-atmosphere interaction is greater at the sea ice

edges and basal layers (Parise et al. 2015). Both the insulating effect of sea ice and the cold and fresh water input on the surface of Southern Ocean contribute to intensify the southern heat gradient, causing more heat to be transported southwards, especially at the latitudes over the ASI edge (Parise 2014).

The presence of sea ice at the poles strongly influences the surface temperature (Raphael et al. 2011). During the melting season (summer), where ocean surface temperatures are warmer, the heat flux from the ocean to the atmosphere is more intense. As they are regions of larger contact with relatively warmer waters, they contribute to the sea ice melting and the release of this heat into the atmosphere. Temperature differences close to the continental edge can be reasonably explained as a direct thermal response to the sea ice distribution.

Our results have also shown a fresh bias near 30° N, which can be related to changes in the Mediterranean Intermediate Water (MIW) flow. The mean cross section of the deep circulation in the Atlantic Ocean shows the presence of the MIW that flows through the Straits of Gibraltar into the Atlantic Ocean (Oppo & Fairbanks 1987). This water is warm and salty from the warm temperatures and high evaporation characteristic of the Mediterranean Sea, so it is denser than the normal surface water and forms a layer about 1–1.5 km deep. Eventually this water will move north to the Greenland Sea, where it will be cooled and will sink, becoming the dense NADW (Giorgi & Lionello 2008). The surface waters of the eastern Mediterranean Sea have a salinity of about 38. As this water is more dense than the Atlantic Ocean surface water (35) so it sinks around 35° N. Carbon isotope records suggest that the influence of Mediterranean Sea extended until the Caribbean Sea during the last glaciation, being the most volumetrically important water mass in the intermediate-depth Atlantic (Oppo & Fairbanks 1987).

CONCLUSIONS

Our study showed that a maximum condition of ASI concentration and thickness has the potential to largely influence on the Southern Ocean stratification, by exporting resulted-melting cold and fresh water towards the equator. By isolating effect, the enhanced buoyance of freshwater also contributes to suppress the vertical heat fluxes, making the Southern Ocean to warm up just below the surface (from 50 to 400 m depth). As cold and fresh surface water is displaced by Ekman transport from Southern Ocean to low latitudes, the heat stored in subsurface layers is released to southern atmosphere. The major changes caused by increased ASI in Southern Ocean and how this climate signal has propagated toward the TAO discussed here are highlighted in a schematic (Figure 5), where the numbers are used to show the sequential changes. The pathways by which the climate signal was transferred via the ocean to the TAO, how this freshwater transport has occurred, in what magnitude and how long it has taken to arrive in the region are suggested to be as follows: **1)** The imposed ASI maxima generated an input of cold and fresh water to the surface of Southern Ocean; **2)** The freshwater ejection from sea ice melting has increased the Southern Ocean buoyance, reducing the vertical heat fluxes and generating a warming in subsurface layers; **3)** As cold and fresh surface water is displaced towards the equator, by Ekman transport (Parise 2014), the heat stored in subsurface layers is then released to southern atmosphere; **4)** and **5)** the northward shift of the colder and fresher water was given by the flows of SAMW and AAIW, when it sinks at the Antarctic Convergence (~50° S) by the process of subduction. SAMW and AAIW are

eventually transported into the subtropical gyre through the eastern boundary, when part of the South Atlantic Current turns northward, feeding the Benguela Current (Figure 5a). The northward transport of SAMW and AAIW from South Atlantic injects these cold and fresh mode/intermediate waters into the subtropical basin; **6)** the climate signal reaches the low latitudes through the equatorial upwelling, eventually warming up on the surface; **7)** in response to the divergent flow at surface, the climate signal spreads out southwards, through the upper branch of subtropical gyre. Our results have showed that TAO was sensitive to the positive extremes of ASI, with significantly changes in ocean temperature (-0.8°C on the surface and +0.2°C between 50–400 m depth) and salinity (-0.2).

Still, we have concluded that 10 years of coupled simulations was enough time to propagate the climate signal generated by ASI positive extremes melting, which has reached the TOA around 2 year later. That is, the oceanic connection between Southern Ocean and TAO is indeed established within the timescale analyzed in the study (i.e., 10 years). Nonetheless, the period needed to completely dissipate the disturbance generated from ASI seems to be longer, being depends on the thermodynamic and dynamic processes of sea ice, the climate mechanisms and feedbacks evolved, and the ocean memory to ASI extremes (Parise 2014, Parise et al. 2015).

Acknowledgments

The authors would like to thank the funding support of Coordenação de Aperfeiçoamento de Pessoal de Nível Superior (CAPES) to the Projects "Advanced Studies in Oceanography of Medium and High Latitudes" (Process 23038.004304/2014-28) and "Use and Development of the Brazilian Earth System Model for the Study of the Ocean-Atmosphere-Cryosphere System in High and Medium Latitudes - BESM/SOAC" (Process 145668/2017-00) and to the funding support of Conselho Nacional de Desenvolvimento Científico e Tecnológico (CNPq) to the Projects "Impactos do Aumento do Gelo Marinho da Antártica no Clima da América do Sul: Simulações por Conjunto x Reanálises" (Process 420406/2016-6) and "Antarctic Modeling Observation System - ATMOS" (Process 443013/2018-7). This publication was also supported by the Fundação de Amparo à Pesquisa e Desenvolvimento Científico e Tecnológico do Maranhão (FAPEMA) (Process 00850/17). L.P.P. is partly funded through a CNPq Scientific Productivity Fellowship (Process 304858/2019-6). The authors also acknowledge the GFDL Coupled Climate Model Development Team for providing a public version of the model and for all technical support.

REFERENCES

AIKEN CM & ENGLAND MH. 2008. Sensitivity of the present-day climate to freshwater forcing associated with Antarctic sea ice loss. J Clim 21(15): 3936-3946.

BITZ CM, GENT PR, WOODGATE RA, HOLLAND MM & LINDSAY R. 2006. The influence of sea ice on ocean heat uptake in response to increasing CO_2. J Clim 19: 2437-2450.

BRYAN F. 1987. Parameter sensitivity of primitive equation ocean general circulation models. J Phys Oceanogr 14: 666-673.

CARTER L, MCCAVE IN & WILLIAMS MJM. 2008. Circulation and water masses of the Southern Ocean: a review. Developments in earth and environmental sciences 8: 85-114.

CARTON JA, CHEPURIN GA & CHEN L. 2018. SODA3: A New Ocean Climate Reanalysis. J Clim 31(17): 6967-6983.

CASAGRANDE F, BUSS RB, NOBRE P & LANFER MA. 2020. An inter-hemispheric seasonal comparison of polar amplification using radiative forcing of a quadrupling CO_2 experiment. Ann Geophys 38: 1123-1138.

CHAI T & DRAXLER RR. 2014. Root Mean Square Error (RMSE) or Mean Absolute Error (MAE)? Geosci Model Dev Discuss 7: 1525-1534.

CHIANG JCH, CHENG W & BITZ CM. 2008. Fast teleconnections to the tropical Atlantic sector from Atlantic thermohaline adjustment. Geophys Res Lett 35: L07704.

COOK AJ, FOX AJ, VAUGHAN DG & FERRIGNO JG. 2005. Retreating glacier fronts on the Antarctic Peninsula over the past half century. Science 308: 541-544.

CURRY R, DICKSON B & YASHAYAEV I. 2003. A change in the freshwater balance of the Atlantic Ocean over the past four decades. Nature 426: 826-829.

DEACON G. 1937. The Hydrology of the Southern Ocean. Cambridge University Press 15: 3-12.

DELWORTH TL ET AL. 2006. GFDL's CM2 global coupled climate models. Part I: formulation and simulation characteristics. J Clim 19(5): 643-674.

EICKEN H, FISCHER H & LEMKE P. 1995. Effects of the snow cover on Antarctic sea ice and potential modulation of its response to climate change. Ann Glaciol 21: 369-376.

FERREIRA DJ, MARSHALL, BITZ CM, SOLOMON S & PLUMB A. 2015. Antarctic ocean and sea ice response to ozone depletion: A two-time-scale problem. J Clim 28: 1206-1226.

FLATO GJ ET AL. 2013. Evaluation of Climate Models. In: Climate Change 2013: The Physical Science Basis. Contribution of Working Group I to the Fifth Assessment Report of the Intergovernmental Panel on Climate Change [Stocker TF, Qin D, Plattner G-K, Tignor M, Allen SK, Boschung J, Nauels A, Xia Y, Bex V and Midgley PM (Eds)]. Cambridge University Press, Cambridge, United Kingdom and New York, NY, USA.

GEORGI DT. 1979. Modal properties of Antarctic Intermediate Water in the southeast Pacific and South Atlantic. J Phys Oceanogr 9: 456-468.

GIANNINI AJCH, CHIANG MA, CANE Y, KUSHNIR & SEAGER R. 2001. The ENSO teleconnection to the tropical Atlantic Ocean: Contributions of the remote and local SSTs to rainfall variability in the tropical Americas. J Clim 14: 4530-4544.

GIORGI F & LIONELLO P. 2008. Climate change projections for the mediterranean region. Glob Planet Change 63: 90-104.

GRIFFIES SM, BÖNING C, BRYAN FO, CHASSIGNET EP, GERDES R, HASUMI H, HIRST A, TREGUIER AM & WEBB D. 2000. Developments in ocean climate modelling. Ocean Modelling 2(34): 123-192.

HAUMANN F, GRUBER N & MÜNNICH M. 2016. Sea-ice transport driving Southern Ocean salinity and its recent trends. Nature 537: 89-92.

HYNDMAN RJ & KOEHLER AB. 2006. Another look at measures of forecast accuracy. Int J Forecast 22(4): 679-688.

JACOBS SS, GIULIVI CF & MELE PA. 2002. Freshening of the Ross Sea during the late 20th century. Nature 297: 386-389.

KIRKMAN C & BITZ CM. 2011. The Effect of the Sea Ice Freshwater Flux on Southern Ocean Temperatures in CCSM3: Deep Ocean Warming and Delayed Surface Warming. J Clim 24: 2224-2237.

KRÖGER J, BUSALACCHI AJ, BALLABRERA-POY J & MALANOTTE-RIZZOLI P. 2005. Decadal variability of shallow cells and equatorial sea surface temperature in a numerical model of the Atlantic. J Geophys Res (Oceans) 110: C12003.

LI X, HOLLAND DM, GERBER EP & YOO C. 2015. Rossby waves mediate impacts of tropical oceans on West Antarctic atmospheric circulation in austral winter. J Clim 28: 8151-8164

LIU J, MARTINSON DG, YUAN X & RIND D. 2002. Evaluating Antarctic sea ice variability and its teleconnections in global climate models. Int. J. Climatol 22: 885-900.

MACKIE S, LANGHORNE PJ, HEORTON HDBS, SMITH IJ, FELTHAM DL & SCHROEDER D. 2020. Sea ice formation in a coupled climate model including grease ice. J Adv Model Earth Syst 12: e2020MS002103.

MAKSYM T, STAMMERJOHN S, ACKLEY S & MASSOM R. 2012. Antarctic Sea Ice: A Polar Opposite? Oceanography 25(3): 140-151.

MAROTZKE J & SCOTT JR. 1999. Convective mixing and thermohaline circulation. J Phys Oceanogr 29: 2962-2970.

MASSOM RA & STAMMERJOHN SE. 2010. Antarctic sea ice change and variability–physical and ecological implications. Polar Sci 4(2): 149-186.

MASSOM RA, STAMMERJOHN SE, LEFEBVRE W, HARANGOZO SA, ADAMS N, SCAMBOS TA, POOK MJ & FOWLER C. 2008. West Antarctic Peninsula sea ice in 2005: Extreme ice compaction and ice edge retreat due to strong anomaly with respect to climate. J Geophys Res 113: C02S20. doi: 10.1029/2007JC004239.

MCCARTNEY AP. 1977. Thule Eskimo Prehistory along Northwestern Hudson Bay. University of Ottawa Press.

MOLINELLI ET. 1981. The Antarctic influence on Antarctic Intermediate Water. J Mar Res 39: 267-293.

MOURA RL ET AL. 2016. An extensive reef system at the Amazon River mouth. Sci Adv 2(4): e1501252.

NADEAU LP, FERRARI R & JANSEN MF. 2019. Antarctic Sea Ice Control on the Depth of North Atlantic Deep Water. J Clim 32: 2537-2551.

OPPO DW & FAIRBANKS RG. 1987. Variability in the deep and intermediate water circulation of the Atlantic Ocean during the past 25,000 years: Northern Hemisphere modulation of the Southern Ocean. Earth Planet Sci Lett 86(1): 1-15.

PARISE CK. 2014. Sensitivity and memory of the current mean climate to increased Antarctic sea ice: The role of sea ice dynamics. PhD. Thesis, National Institute for Space Research (INPE), 218 p.

PARISE CK, PEZZI LP, HODGES KI & JUSTINO F. 2015. The Influence of Sea Ice Dynamics on the Climate Sensitivity and Memory to Increased Antarctic Sea Ice. J Clim 28: 9642-9668.

PARKINSON CA. 2019. 40–y record reveals gradual Antarctic sea ice increases followed by decreases at rates far exceeding the rates seen in the Arctic. Proceedings of the National Academy of Sciences 116(29): 14414-14423.

PETERSON RG & STRAMMA L. 1991. Upper-level circulation in the South Atlantic Ocean. Prog Oceanogr 26: 1-73.

PEZZI LPRBS, ACEVEDO O, WAINER IM, MATA M, GARCIA CAE & CAMARGO R. 2009. Multiyear measurements of the oceanic and atmospheric boundary layers at the Brazil-Malvinas confluence region, J Geophys Res 114: D19103.

PEZZI LP & CAVALCANTI IFA. 2001. The relative importance of ENSO and tropical Atlantic sea surface temperature anomalies for seasonal precipitation over South America: A numerical study. Clim Dyn 17: 205-212.

PEZZI LP, SOUZA RB, FARIAS PC, ACEVEDO O & MILLER AJ. 2016. Air-sea interaction at the Southern Brazilian Continental Shelf: In situ observations. J Geophys Res (Ocean) 121.

PEZZI LP ET AL. 2021. Oceanic eddy-induced modifications to air–sea heat and CO_2 fluxes in the Brazil-Malvinas Confluence. Sci Rep 11: 10648.

PIOLA AR & GEORGI DT. 1982. Circumpolar properties of Antarctic Intermediate Water and Subantarctic Mode Water. Deep Sea Res 29: 687-711.

PIOLA AR & GORDON AL. 1989. Intermediate water in the southwestern South Atlantic. Deep Sea Res 36: 1-16.

PURICH A & ENGLAND MH. 2019. Tropical teleconnections to Antarctic sea ice during austral spring 2016 in coupled pacemaker experiments. Geophys Res Lett 46: 6848-6858.

RANDALL D ET AL. 2007. Climate Models and Their Evaluation. In: Climate Change 2007: The Physical Science Basis. Contribution of Working Group I to the Fourth Assessment Report of the Intergovernmental Panel on Climate Change [Solomon S, Qin D, Manning M, Chen Z, Marquis M, Averyt KB, Tignor M and Miller HL (Eds)]. Cambridge University Press, Cambridge, United Kingdom and New York, NY, USA.

RAPHAEL MN, HOBBS W & WAINER I. 2011. The effect of Antarctic sea ice on the Southern Hemisphere atmosphere during the southern summer. Clim Dyn 36: 1403-1417.

RAYNER NA, PARKER DE, HORTON EB, FOLLAND CK, ALEXANDER LV, ROWELL, DP, KENT EC & KAPLAN A. 2003. Global analyses of sea surface temperature, sea ice, and night marine air temperature since the late nineteenth century. J Geophys Res Atmos: 108 (D14): 1-37.

SCHMITZ WJ JR & RICHARDSON PL. 1991. On the sources of the Florida Current. Deep Sea Res. Part I Oceanogr Res Pap 38: S379-S409.

SLOYAN BM & RINTOUL SR. 2001.Circulation, renewal, and modification of Antarctic mode and intermediate water. J Phys Oceanogr 31: 1005-1030.

STAMMERJOHN S ET AL. 2012. Regions of rapid sea ice change: An inter-hemispheric seasonal comparison. Geophys Res Lett 39(6).

STRAMMA L & PETERSON RG. 1990. The South Atlantic Current. J Phys Oceanogr 20: 846-859.

STUECKER MF ET AL. 2018. Polar amplification dominated by local forcing and feedbacks. Nat Clim Chang 8: 1076-1081.

TAYLOR K, WILLIAMSON D & ZWIERS F. The Sea Surface Temperature and Sea-ice Concentration Boundary Conditions for AMIP II Simulations. 2000. PCMDI report: Program for Climate Model Diagnosis and Intercomparison, 28 p.

THOMAS DN & DIECKMANN GS (Eds). 2010. Sea Ice. 2. ed., Wiley, 621 p.

TOGGWEILER JR & SAMUELS B. 1995. Effect of sea ice on the salinity of Antarctic bottom waters. J Phys Oceanogr 25: 1980-1997.

UTIDA G ET AL. 2019. Tropical South Atlantic influence on Northeastern Brazil precipitation and ITCZ displacement during the past 2300 years. Sci Rep 9: 1698.

WALLACE JM & GUTZLER DS. 1981. Teleconnections in the Geopotential Height Field during the Northern Hemisphere Winter. Mon Weather Rev 109: 784-812.

WILLIAMS R, ROUSSENOV V & FOLLOWS M. 2006. Nutrient streams and their induction into the mixed layer. Global Biogeochem Cycles 20: 10.1029/2005GB002586.

WU L, HE F, LIU Z & LI C. 2007. Atmospheric teleconnections of tropical Atlantic variability: interhemispheric, tropical–extratropical, and cross-basin interactions. J Clim 20: 856-870.

YOON JH & ZENG N. 2010. An Atlantic influence on Amazon rainfall. Clim Dyn 34: 249-264.

SUPPLEMENTARY MATERIAL

Figure S1.

How to cite
TORRES ALR, PARISE CK, PEZZI LP, DOS SANTOS QUEIROZ MG, MACHADO AMB, CERVEIRA GS, CORREIA GS, BARBOSA WL, DE LIMA LG & SUTIL UA. 2022. Lagged response of Tropical Atlantic Ocean to cold and fresh water pulse from Antarctic sea ice melting. An Acad Bras Cienc 94: e20210800. DOI 10.1590/0001-3765202220210800.

Manuscript received on May 28, 2021;
accepted for publication on September 28, 2021

ANA LAURA R. TORRES[1]
https://orcid.org/0000-0003-0155-4059

CLAUDIA K. PARISE[1]
https://orcid.org/0000-0002-9466-788X

LUCIANO P. PEZZI[2]
https://orcid.org/0000-0001-6016-4320

MICHELLY G. DOS SANTOS QUEIROZ[1]
https://orcid.org/0000-0002-4732-7911

ADILSON M.B. MACHADO[1]
https://orcid.org/0000-0002-4838-6913

GABRIEL S. CERVEIRA[1]
https://orcid.org/0000-0001-8016-4328

GUSTAVO S. CORREIA[3]
https://orcid.org/0000-0003-0088-3264

WESLEY L. BARBOSA[1]
https://orcid.org/0000-0002-9279-5626

LEONARDO G. DE LIMA[4]
https://orcid.org/0000-0001-7449-8639

UESLEI A. SUTIL[2]
https://orcid.org/0000-0002-7150-536X

[1]Universidade Federal do Maranhão (UFMA), Departamento de Oceanografia e Limnologia (DEOLI), Laboratório de Estudo e Modelagem Climática (LACLIMA), Avenida dos Portugueses, 1966, Vila Bacanga, 65080-805 São Luís, MA, Brazil

[2]Instituto Nacional de Pesquisas Espaciais (INPE), Laboratório de Estudos do Oceano e da Atmosfera (LOA), Divisão de Observação da Terra e Geoinformática (DIOTG), Avenida dos Astronautas, 1758, Jardim da Granja, 12227-010 São José dos Campos, SP, Brazil

[3]Programa de Pós-Graduação em Geociências (PPGGEO), Universidade Federal do Rio Grande do Sul (UFRGS), Instituto de Geociências, Av. Bento Gonçalves, 9599, Campus Agronomia, 91501-970 Porto Alegre, RS, Brazil

[4]Universidade Federal do Maranhão (UFMA), Departamento de Oceanografia e Limnologia (DEOLI), Laboratório de Estudos de Oceanografia Geológica (LEOG), Avenida dos Portugueses, 1966, Vila Bacanga, 65080-805 São Luís, MA, Brazil

Correspondence to: **Claudia Klose Parise**
E-mail: claudiakparise@gmail.com

Author contributions

Ana Laura Torres processed the climate data, applied the methods and analyzes and wrote the manuscript. Cláudia Parise performed the conceptualization of the manuscript, provided the numerical climate data, helped writing the manuscript, supervised the work. Luciano Pezzi has contributed with the infrastructure needed for carrying out the numerical experiments and helped to write the manuscript. Michelly Queiroz, Adilson Machado, Gabriel Cerveira, Gustavo Correia, Wesley Barbosa and Ueslei Sutil were involved in the methodology and data processing. Leonardo de Lima helped with the creation and consolidation of the Laboratory for Climate Studies and Modelling (LaClima) at the Department of Limnology and Oceanography in the Federal University of Maranhão where most analyzes could be conducted.